

Supplementary Materials for  
**Airborne fine particles drive H1N1 viruses deep into the lower respiratory tract and distant organs**

Zheng Dong *et al.*

Corresponding author: Sijin Liu, [sjliu@rcees.ac.cn](mailto:sjliu@rcees.ac.cn); Min Fang, [fangm@im.ac.cn](mailto:fangm@im.ac.cn)

*Sci. Adv.* **9**, eadf2165 (2023)  
DOI: 10.1126/sciadv.adf2165

**This PDF file includes:**

Figs. S1 to S13  
Table S1

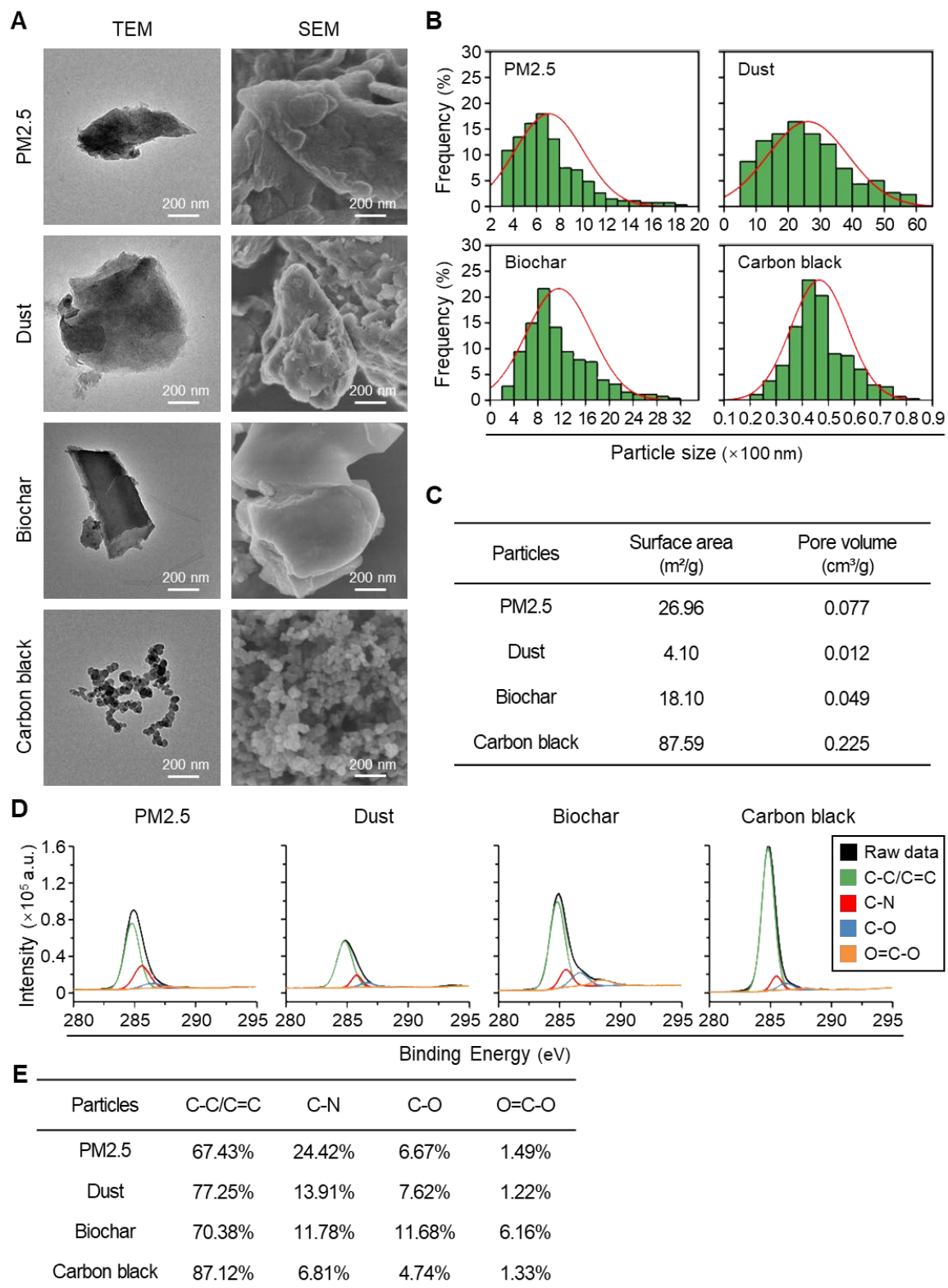


**Fig. S1. Physicochemical characterization of various airborne fine particles (AFPs). (A)**

Representative transmission electron microscopy (TEM, left panel) and scanning electron microscopy (SEM, right panel) images of PM2.5, dust, biochar and carbon black. **(B)** Histograms show the size distribution profiles of different AFPs with Gaussian curve fitting. **(C)** Brunauer-Emmett-Teller (BET) analysis of surface area and micropore volume. **(D)** X-ray photoelectron spectroscopy (XPS) analysis of the surface composition of AFPs **(E)** Quantification of the carbon-based functional groups in AFPs (range: 0-100%).

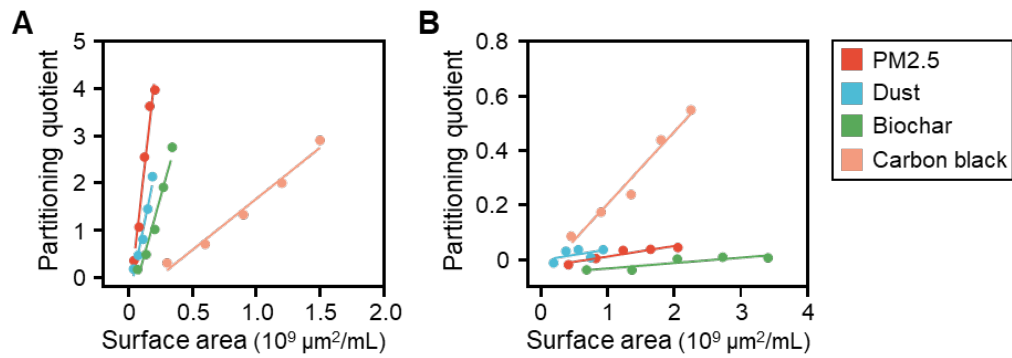


**Fig. S2. Determination of the hydrophilicity and hydrophobicity of AFPs.** Linear regression of the partitioning quotient (PQ) of (A) Nile Blue (NB) and (B) Rose Bengal (RB) against the surface areas of AFPs. NB is a hydrophilic dye. The slope in (A) indicates the relative hydrophilicity among these AFPs. RB is a hydrophobic dye. The slope in (B) indicates the relative hydrophobicity among these AFPs.

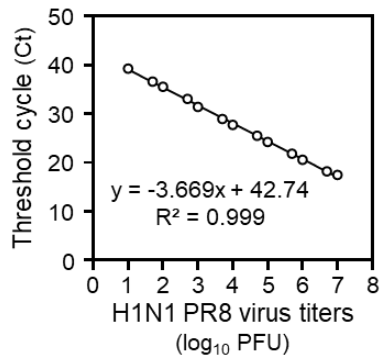


**Fig. S3. Standard curve for obtaining the viral genomic equivalent titers.** The standard curve of viral titers developed from SYBR green-based qRT-PCR analysis of viral matrix protein 1 (*M1*) gene, which was generated by 10-fold serial dilution of virus stocks ( $n = 3$ ). Coefficient of determination ( $R^2$ ) and slope of the regression curves are shown.

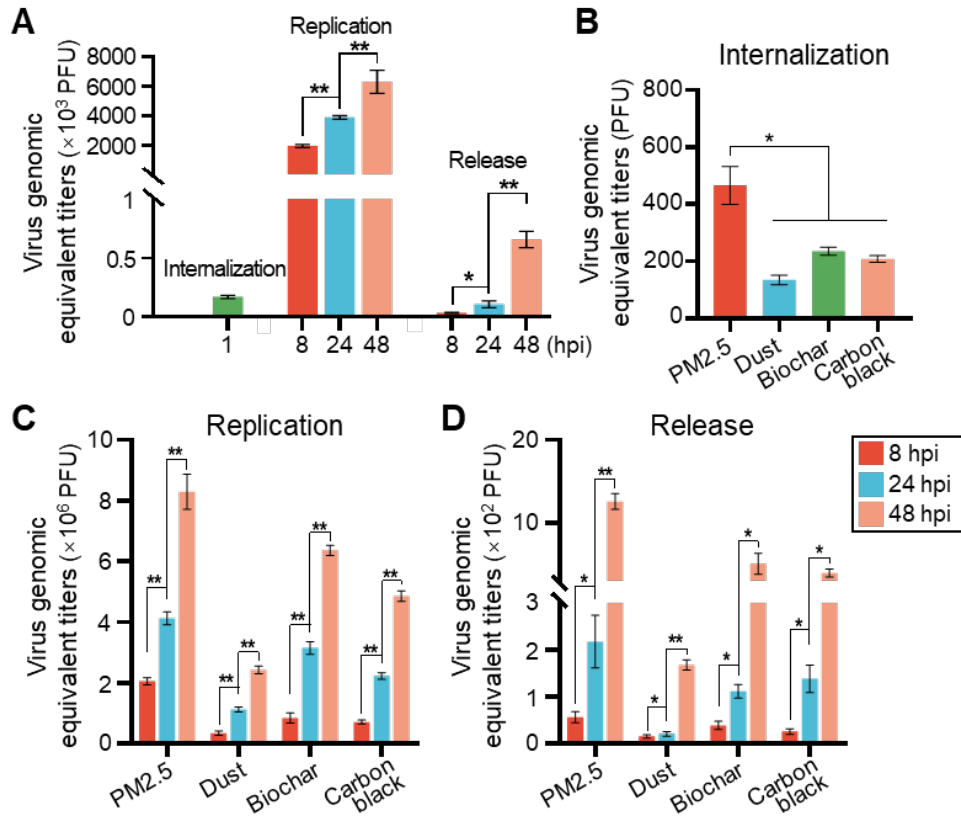


**Fig. S4. Viruses loaded on AFPs remain infectious in primary human small airway epithelial cells (hSAECs).** (A) Quantification of internalized, replicated and released viruses in hSAECs infected with solo viruses (at 200 plaque forming unit, PFU) through SYBR green-based qRT-PCR assays ( $n = 4$ ). (B to D) Quantification of (B) internalized, (C) replicated and (D) released viruses in AFP-borne virus-infected hSAECs ( $n = 4$ ). Replication and release of viruses were quantified at 8, 24 and 48 hpi. (\*) indicates  $P < 0.05$ , and (\*\*) denotes  $P < 0.001$ , as indicated.

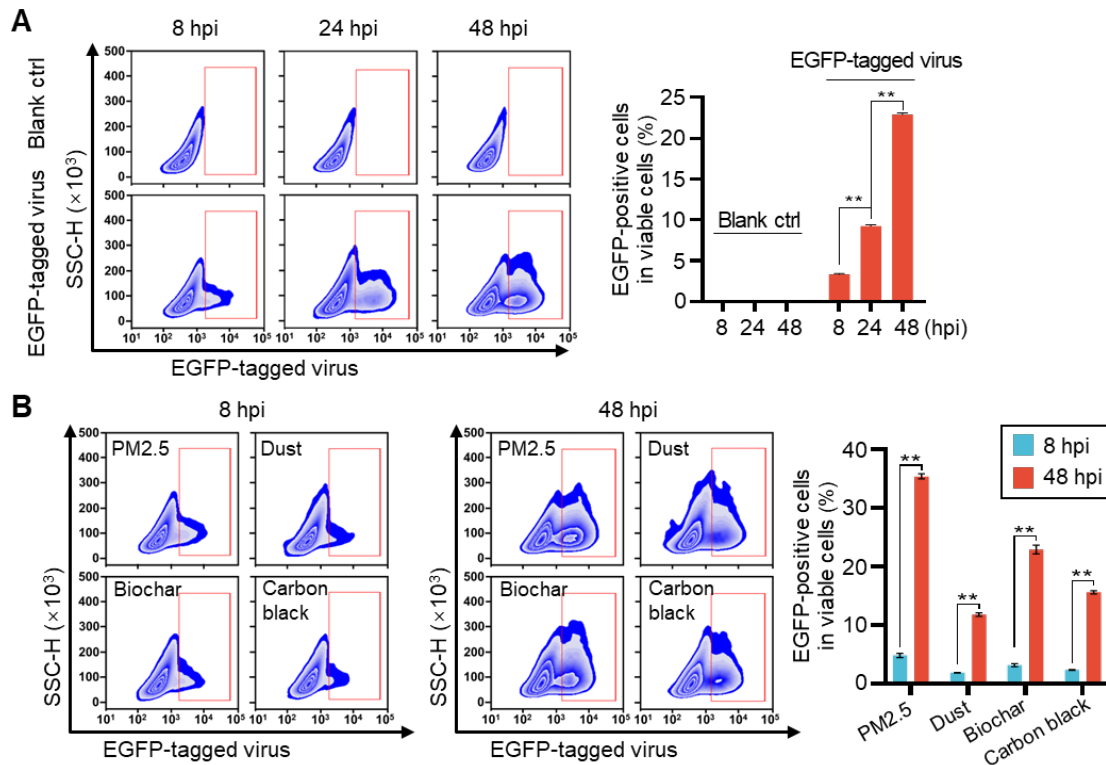


**Fig. S5. Flow cytometry analysis of AFP-borne virus infection.** (A) Flow cytometry data (left panel) and quantitative analysis (right panel) of A549 cells infected with enhanced green fluorescent protein (EGFP)-tagged viruses (1000 PFU) at 8, 24 and 48 hpi ( $n = 4$ ). (B) Flow cytometry data and quantitative analysis of A549 cells infected with 50  $\mu\text{g/mL}$  EGFP-tagged virus-laden AFPs at 8 and 48 hpi ( $n = 4$ ). (\*) indicates  $P < 0.05$ , and (\*\*) denotes  $P < 0.001$ , as indicated.

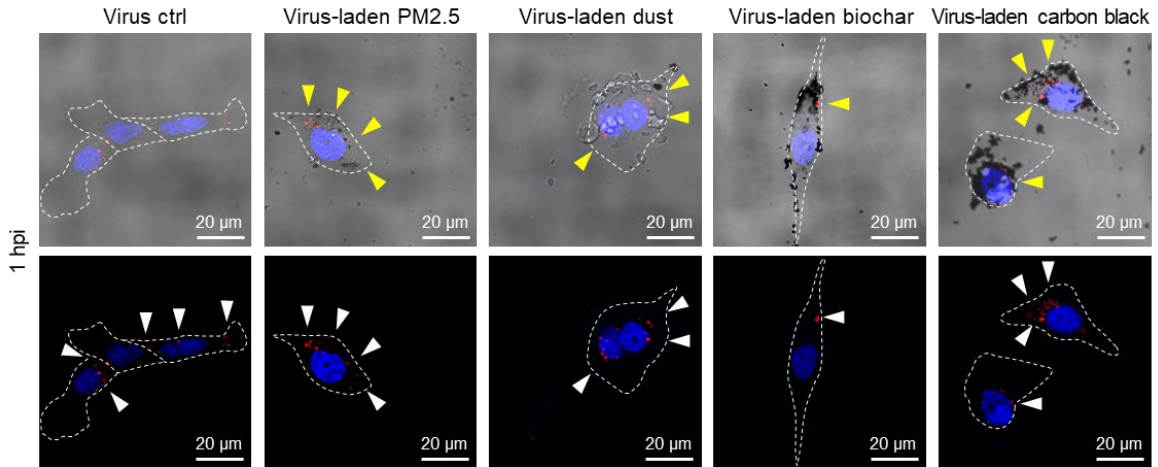


**Fig. S6. AFPs transport viruses into target cells.** Representative merged images of bright-field and immuno-fluorescent staining (upper panel) and confocal images (lower panel) of hSAECs infected with solo viruses (at 200 PFU) or 50 μg/mL virus-laden AFPs for 1 h. Intracellular virions are stained with an anti-hemagglutinin (HA) antibody (red). Cell nuclei are stained with DAPI in blue. Cell morphology is indicated by dashed line. Yellow arrowheads denote the location of AFPs, and white arrowheads indicate viruses.



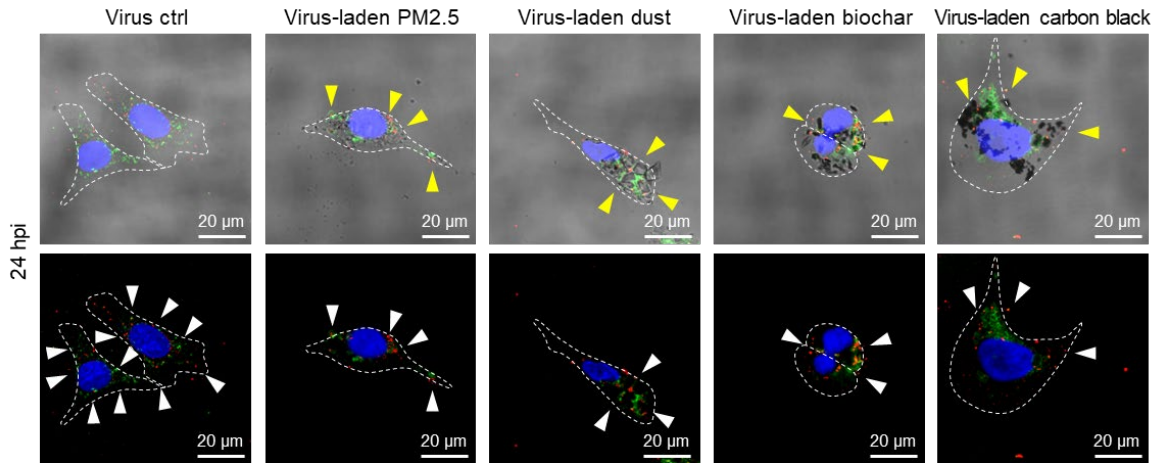


**Fig. S7. AFPs favor progeny virion budding.** Representative merged images of bright-field and immuno-fluorescent staining (upper panel) and confocal images (lower panel) of hSAECs infected with solo viruses (at 200 PFU) or 50 µg/mL virus-laden AFPs for 24 h. Virions are stained with an anti-HA antibody (red), and lipid rafts are stained with an anti-flotillin 1 antibody (green). Cell nuclei are stained with DAPI in blue. Cell morphology is indicated by dashed line. Yellow arrowheads denote the location of AFPs, and white arrowheads indicate virions.

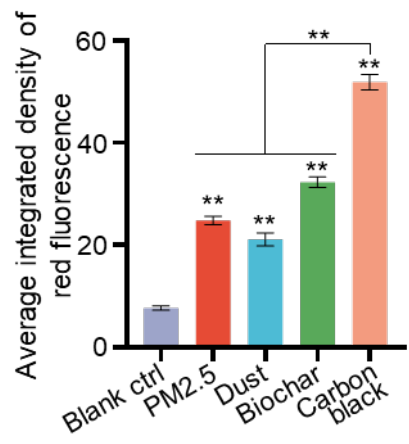


**Fig. S8.** The quantitative analysis of red fluorescence (Evans blue) of A549 cells treated with 20  $\mu\text{g}/\text{mL}$  AFPs for 24 h. The immunofluorescent intensity was quantified using the ImageJ software by randomly selecting more than 20 cells. (\*\*) denotes  $P < 0.001$ , relative to blank control, or as indicated.

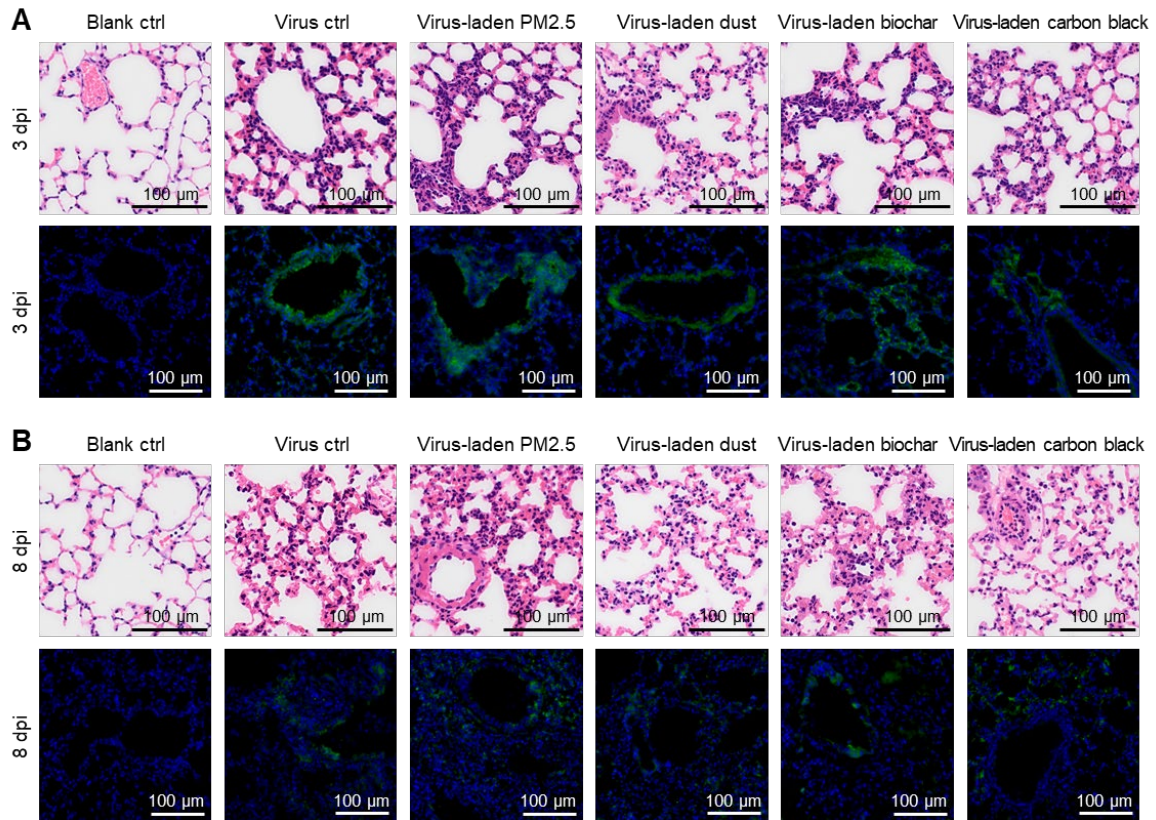


**Fig. S9. Virus-laden AFPs cause inflammation and damage in the lung. (A and B)** Representative hematoxylin and eosin (H&E)-stained lung sections (upper panel) and confocal images of lung sections stained with an anti-HA antibody (lower panel, green) from mice treated with PBS (blank control), solo viruses or 200  $\mu\text{g}/\text{kg}$  body weight virus-laden AFPs at (A) 3 and (B) 8 days post infection (dpi). Cell nuclei are stained with DAPI (blue).

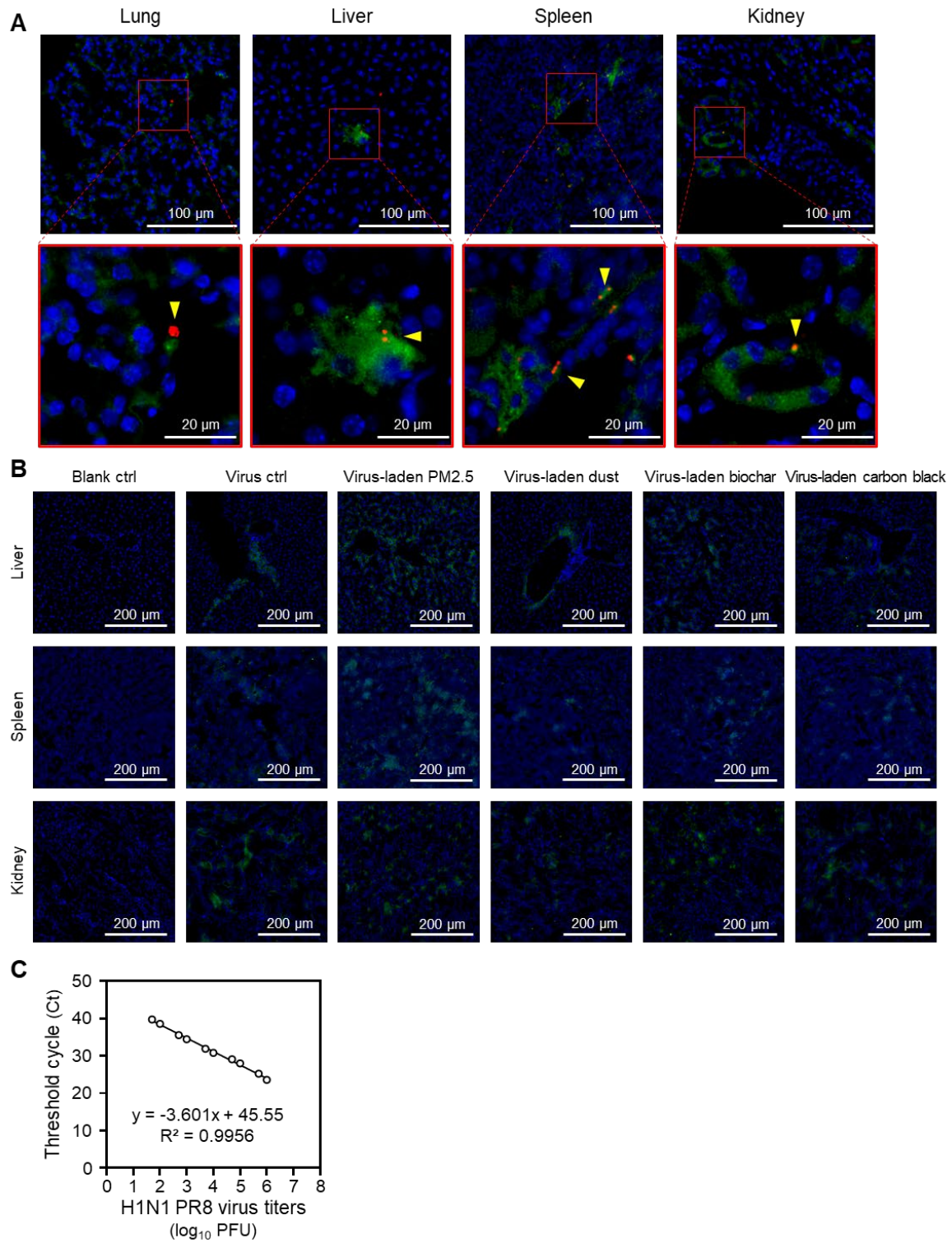


**Fig. S10. AFPs facilitate the spread of viruses into distant organs.** (A) Representative immunofluorescent staining of lung sections obtained from mice treated with virus-laden

polystyrene particles at 1 dpi, and liver, spleen and kidney sections at 3 dpi. Polystyrene particles (red) are colocalized with viruses (green) in these organs. Viruses are stained with an anti-HA antibody (green), and cell nuclei are stained with DAPI (blue). **(B)** Representative confocal images of liver, spleen and kidney sections obtained from mice treated with solo viruses or virus-laden AFPs at 3 dpi. Viruses are stained with an anti-HA antibody (green), and cell nuclei are stained with DAPI (blue). **(C)** Standard curve of viral titers generated from TaqMan qRT-PCR analysis of viral polymerase acidic protein (*PA*) gene. The standard curve was generated by 10-fold serial dilution of virus stocks ( $n = 3$ ). This method is developed for *in vivo* assessment of viral distribution. Coefficient of determination ( $R^2$ ) and slope of the regression curves are shown.

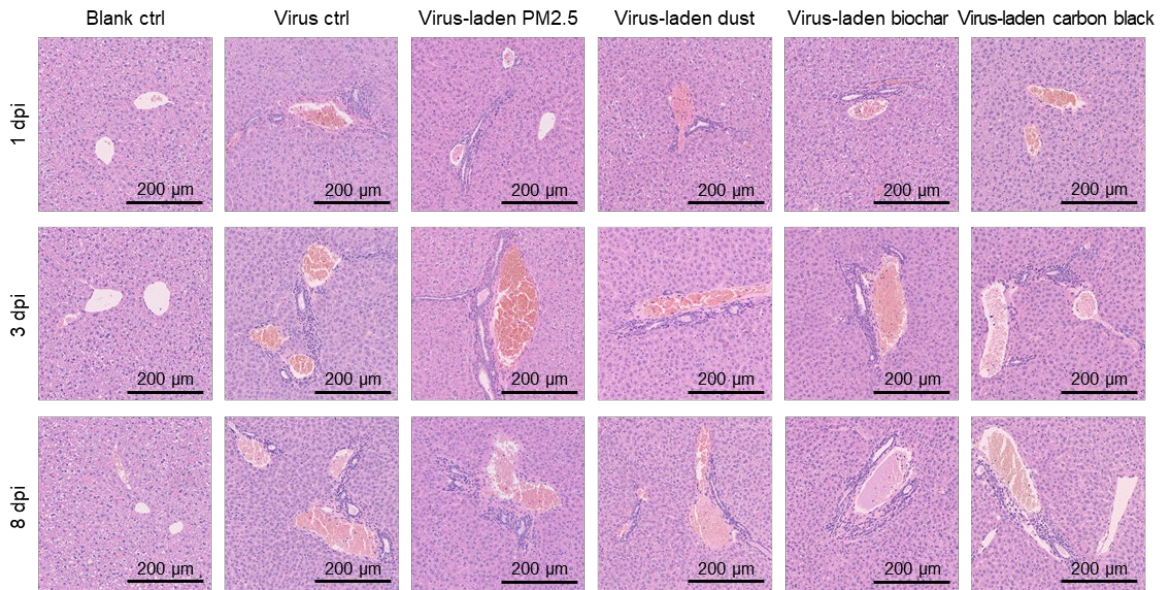


**Fig. S11. Histological examination of the liver.** Representative H&E-stained liver sections from mice treated with PBS (blank control), solo viruses and virus-laden AFPs at 1, 3 and 8 dpi.

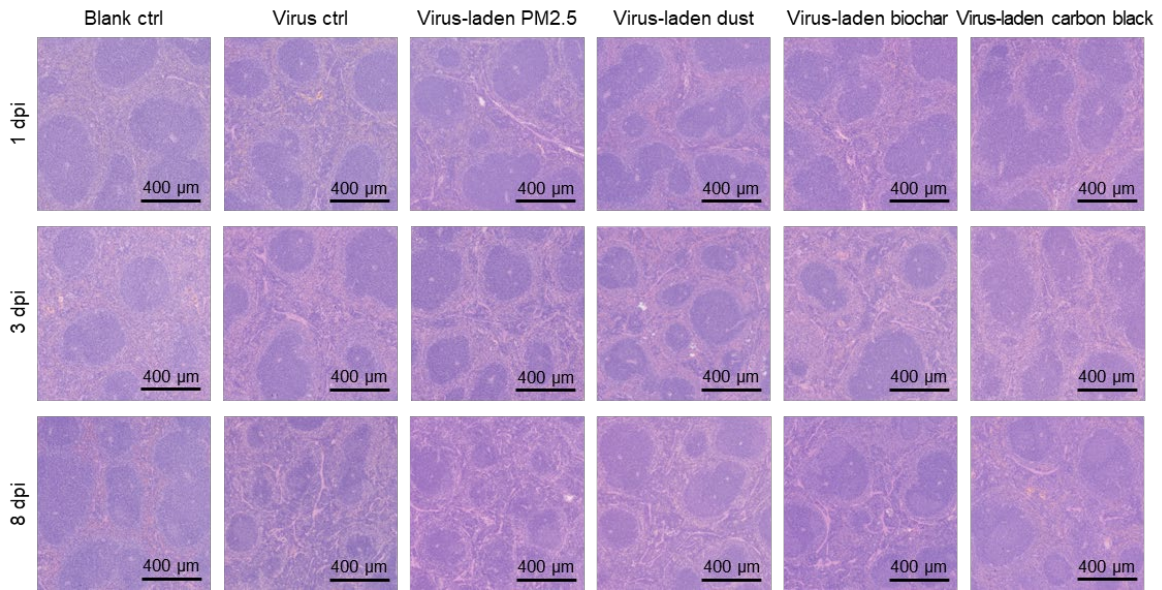


**Fig. S12. Histological examination of the spleen.** Representative H&E-stained spleen sections from mice treated with PBS (blank control), solo viruses and virus-laden AFPs at 1, 3 and 8 dpi.

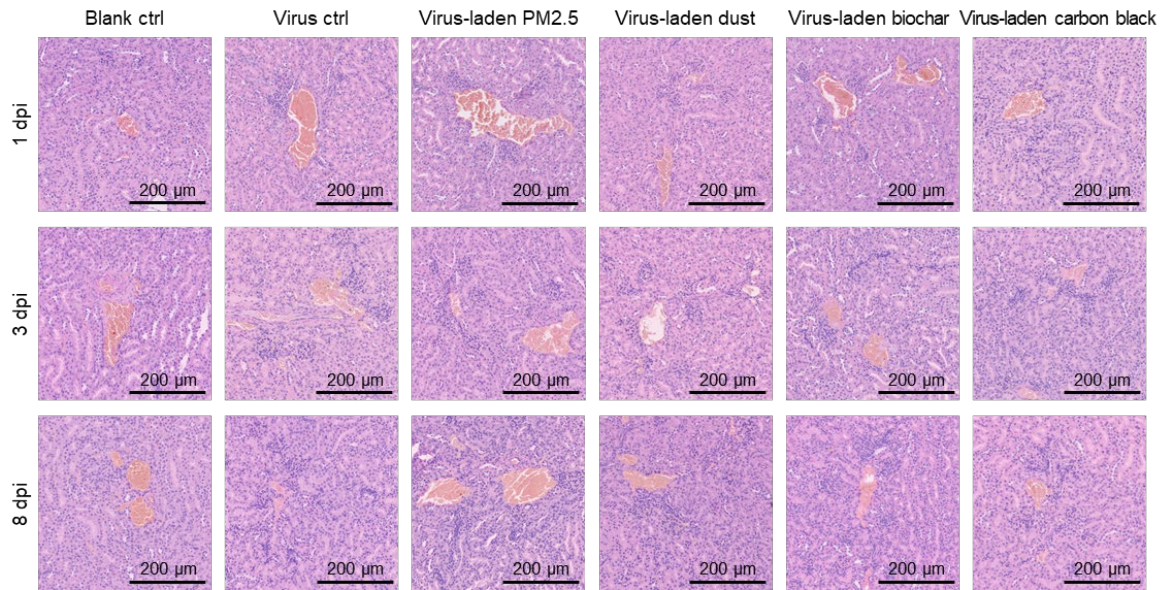


**Fig. S13. Histological examination of the kidney.** Representative H&E-stained kidney sections from mice treated with PBS (blank control), solo viruses and virus-laden AFPs at 1, 3 and 8 dpi.



**Table S1. Primers sequences used in this study.**

<b>Methods</b>	<b>Genes</b>	<b>Sequences (5'-3')</b>
SYBR green	PR8-M1-F	AAGACCAATCCTGTCACCTCTGA
qRT-PCR analysis	PR8-M1-R	CAAAGCGTCTACGCTGCAGTCC
TaqMan	PR8-PA-F	CGGTCCAAATTCCTGCTGA
qRT-PCR analysis	PR8-PA-R	CATTGGGTTTCCTTCCATCCA
	PR8-PA probe	6-FAM-CCAAGTCATGAAGGAGAGGGAATACCGCT-TAMRA